OCEANOGRAPHY

Deep ocean microbial communities produce more stable dissolved organic matter through the succession of rare prokaryotes

Richard LaBrie[1,2]*†, Bérangère Péquin[1,2], Nicolas Fortin St-Gelais[1,2], Igor Yashayaev[3], Jennifer Cherrier[4], Yves Gélinas[5], François Guillemette[2,6], David C. Podgorski[7], Robert G. M. Spencer[8], Luc Tremblay[9], Roxane Maranger[1,2]

The microbial carbon pump (MCP) hypothesis suggests that successive transformation of labile dissolved organic carbon (DOC) by prokaryotes produces refractory DOC (RDOC) and contributes to the long-term stability of the deep ocean DOC reservoir. We tested the MCP by exposing surface water from a deep convective region of the ocean to epipelagic, mesopelagic, and bathypelagic prokaryotic communities and tracked changes in dissolved organic matter concentration, composition, and prokaryotic taxa over time. Prokaryotic taxa from the deep ocean were more efficient at consuming DOC and producing RDOC as evidenced by greater abundance of highly oxygenated molecules and fluorescent components associated with recalcitrant molecules. This first empirical evidence of the MCP in natural waters shows that carbon sequestration is more efficient in deeper waters and suggests that the higher diversity of prokaryotes from the rare biosphere holds a greater metabolic potential in creating these stable dissolved organic compounds.

INTRODUCTION

The ocean holds as much carbon in its dissolved organic matter (DOM) pool as the atmosphere does CO_2, with most oceanic dissolved organic carbon (DOC) resisting biodegradation for millennia (*1*) thereby contributing to climate stability. Prokaryotes are suggested to produce most of this long-lived DOM either through successive and relatively rapid (days to months) transformation of labile DOC to intrinsically refractory DOC (RDOC) (*2*–*4*) or by consuming compounds down to an energetically unprofitable threshold (via "dilution") (*5*, *6*). Some authors argue that both microbial carbon sequestration pathway processes are part of the microbial carbon pump (MCP) (*7*), whereas others refer to the MCP as the recalcitrance hypothesis only (*8*, *9*) as described in the original seminal paper (*4*). Here, we will present them as two separate hypotheses, as their relative importance to carbon sequestration may differ in space and over time, particularly in a rapidly changing ocean (*8*, *10*). On the basis of the recalcitrance hypothesis, the MCP may represent the equivalent of 27 to 58% of the particulate flux at 2000 m created by the more established biological carbon pump (*9*), thus making it another major carbon sequestration pathway. Indirect evidence using bacterial biomarkers shows that large fractions of marine DOC and nitrogen are of microbial origin (*11*–*13*). Moreover, indirect evidence of the MCP using $\delta^{13}C$ signatures of hydrocarbons suggests the role of microbes in storing large amounts of RDOC in ocean sediments, with overlying anoxic waters, influencing Proterozoic climate (*14*). However, direct evidence of the modern MCP has only been demonstrated in artificially amended waters (*2*, *3*, *15*) and remains untested in a natural setting.

DOM reprocessing is dependent on the prokaryotic community composition as different taxa are known to prefer certain types of molecular compounds (*16*, *17*). However, the prokaryotic taxa involved in the RDOC sequestration through the MCP have not been identified. Community composition differs among major ocean strata (*18*), and it is likely that some communities may be more efficient than others at producing refractory DOM. Deep ocean prokaryotic communities are very diverse and harbor a rich rare biosphere (*19*, *20*), a group of individual taxa that represents less than 0.1% of total abundance. Taxa in the rare biosphere likely have a myriad of alternative metabolic pathways to transform DOM and may serve as a seed bank (*21*) where rare taxa become abundant once labile substrates are replaced by semilabile ones. However, the diversity of and role played by the rare biosphere among ocean layers influencing carbon sequestration efficiency of the MCP remain unknown.

The Labrador Sea is a region of deep convective mixing, described as one of the tipping points of the Earth's climate system because of its role in O_2 and CO_2 export to the deep ocean (*22*). The efficiency of this CO_2 entrainment (*23*) is influenced by interannual variations in convective mixing depth, which fluctuates between the mesopelagic and bathypelagic zones (*24*). In addition to entraining gases, surface DOM will also reach different strata, where it will be exposed to distinctive prokaryotic communities (*25*). The uniqueness of the deep convective mixing in the Labrador Sea, which fluctuates among years and can reach down to 2500 m (*26*), makes it a key and

[1]Département des sciences biologiques, Université de Montréal, Pavillon MIL C. P. 6128, succ. Centre-ville, Montréal, QC H3C 3J7, Canada. [2]Groupe de recherche interuniversitaire en limnologie et environnement aquatique (GRIL), Université de Montréal, C. P. 6128, succ. Centre-ville, Montréal, QC H3C 3J7, Canada. [3]Department of Fisheries and Ocean Canada, Bedford Institute of Oceanography, 1 Challenger Dr., Dartmouth, NS B2Y 4A2, Canada. [4]Department of Earth and Environmental Sciences, Brooklyn College–The City University of New York, 2900 Bedford Avenue, Brooklyn, NY 11210, USA. [5]Geotop and Department of Chemistry and Biochemistry, Concordia University, 7141 Sherbrooke W., Montréal, QC H4B 1R6, Canada. [6]Département des sciences de l'environnement, Université du Québec à Trois-Rivières, 3351 Boulevard des Forges, Trois-Rivières, QC G8Z 4M3, Canada. [7]Pontchartrain Institute for Environmental Sciences, Department of Chemistry, The University of New Orleans, 2000 Lakeshore Dr., New Orleans, LA 70148, USA. [8]National High Magnetic Field Laboratory, Geochemistry Group, Department of Earth, Ocean and Atmospheric Science, Florida State University, Tallahassee, FL 32306, USA. [9]Département de chimie et biochimie, Université de Moncton, 18, avenue Antonine-Maillet, Moncton, NB E1A 3E9, Canada.
*Corresponding author. Email: richard.labrie90@gmail.com
†Present address: Interdisciplinary Environmental Research Centre, TU Bergakademie Freiberg, Akademiestraße 6, 09599 Freiberg, Germany.

ideal location to (i) test the efficiency of epi-, meso-, and bathypelagic communities in consuming DOC and stimulating the MCP in a natural setting and (ii) identify which prokaryotic taxa are involved in the production of RDOC. Furthermore, our experimental design also assessed the potential effect of eddies, which are common almost everywhere in the global ocean (*27*), on the DOM-prokaryotic interactions in carbon sequestration, making our findings more broadly applicable.

RESULTS

DOC degradation

Deep convective mixing was emulated by inoculating 8 liters of 0.2-μm filtered surface water with prokaryotic communities with 2 liters of water collected in the epipelagic (20 m), mesopelagic (500 m), and bathypelagic (1500 m) filtered at 53 μm in duplicate for three treatments. To track DOM and prokaryotic changes among treatments, microcosms were sampled frequently (from daily to monthly) and in considerable detail (see Materials and Methods) for the first 92 days, with final DOC concentrations verified after ~1.5 years of incubation. In terms of DOC consumption among treatments, the measured DOC decay constant (k) was slightly higher in the bathypelagic treatment (0.099 ± 0.037 days^{-1}) but was not significantly different [analysis of variance (ANOVA), $F_{2,56} = 0.738$, $P = 0.48$] from the k in the epi- and mesopelagic treatments (0.059 ± 0.016 days^{-1} and 0.061 ± 0.023 days^{-1}, respectively). As a result, the bathypelagic treatment reached a plateau baseline of 53 ± 1 μmol C liter^{-1} DOC at 50 days of incubation as compared to around 85 days for the epi- and mesopelagic treatments (Fig. 1A). A slight increase in DOC concentration was observed between 31 and 62 days, possibly due to chemoautotrophy, but was overridden by consumption and declined toward the end of the incubation (Fig. 1 and table S1). There was a rapid growth of prokaryotes in the surface treatments followed by a fast decline, probably in response to the labile DOM addition and its exhaustion, respectively (fig. S1) (*28*). In contrast, cell counts remained low in deeper treatments (meso- and bathypelagic) and peaked later, but prokaryotes were still very active, resulting in a higher specific biomass production (ANOVA with post hoc Tukey test, $P < 0.05$; Fig. 1B). This result suggests a higher affinity to this fresher DOM by deeper prokaryotic taxa.

DOM transformation: Emergence of recalcitrant molecules

Different DOM patterns of assigned molecular formulae (MF) using Fourier transform ion cyclotron resonance mass spectrometry with negative electrospray ionization mode (ESI-FT-ICR-MS) among treatments were identified after 92 days of incubation (Fig. 2, A to C). Overall changes among broad DOM categories were observed: unsaturated high oxygen MF increased and unsaturated low oxygen MF decreased in the deeper treatments (Fig. 2, D to F). In contrast, carboxyl-rich alicyclic molecules (CRAM) decreased by up to 5% in all treatments (fig. S3C). Nevertheless, CRAM still represented about 65% of the total MF signal. When we assessed shifts over time using Van Krevelen plots, less oxygenated MF were largely consumed (dark blue dots) in both the bathypelagic and mesopelagic treatments with similar O/C ranges of 0.2 to 0.4 and 0.2 to 0.3, respectively, whereas the epipelagic treatment showed a smaller consumption of O-poor molecules (Fig. 2). DOM with a net positive signal increase (Fig. 2, A to C; dark red dots) by mesopelagic prokaryotic communities had O/C ratios of between 0.4 and 0.7 and H/C ratios of 1.1 and 1.6, whereas the ranges of these ratios were broader in the bathypelagic treatment at 0.4 to 0.9 and 0.7 to 1.6, respectively. This general pattern was observed after 20 days of incubation (fig. S2, A to C) and became more pronounced over time (fig. S3A; ANOVA with post hoc Tukey test, $P < 0.05$), suggesting the iterative process of creating relatively oxidized and stable molecules, particularly in the deep ocean. However, the nominal oxidation state of carbon (NOSC) increased only in the bathypelagic treatment (fig. S3B; ANOVA with post hoc Tukey test, $P < 0.05$). The qualitative changes in MF does not necessarily support the net production of more stable molecules, particularly given the overall DOC consumption, but changes in the fluorescence signal of different DOM components provided semiquantitative evidence of an increase in more refractory material over the course of incubations. The FDOM component $F_{\lambda em}486$ increased over time in the deeper treatments (fig. S3C; ANOVA with post hoc Tukey test, $P < 0.05$) and in all treatments after 548 days (ANOVA with post hoc Tukey test, $P < 0.05$), and the component $F_{\lambda em}392$ increased over time in all treatments (fig. S3D; ANOVA with post hoc Tukey test, $P < 0.05$). Combined, these results support the production or alteration of compounds into more stable molecules by prokaryotes in the three oceanic strata we looked at, but especially by those inoculated by communities from the deeper meso- and bathypelagic ocean.

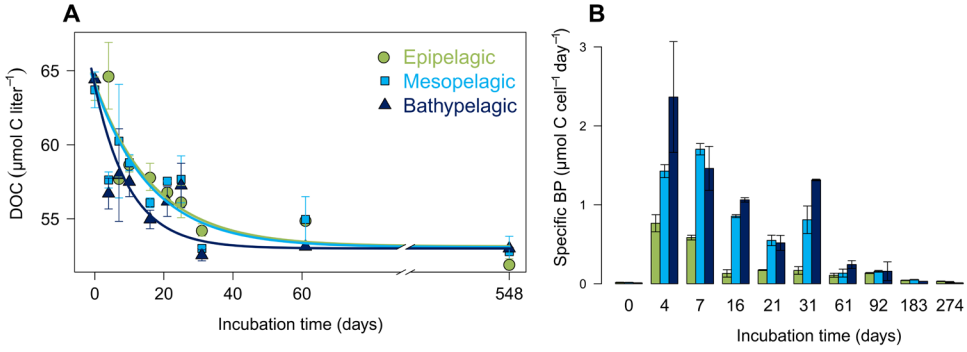

Fig. 1. Time series of DOC concentration and specific biomass production. (**A**) Bulk DOC concentration in μmol C liter^{-1} as a function of incubation time (days). The DOC decay curves were performed using a two pools multi-G approach. The *x* axis was truncated to better visualize all data points. (**B**) Specific production rates as a function of incubation time. Specific production rates, i.e., biomass production (BP) normalized to abundance, were at least twofold higher in the bathypelagic treatment as compared to the epipelagic treatment during the first 2 months of the experiment but were generally similar to the mesopelagic treatment. Error bars represent the mean absolute deviation between treatment duplicates in (A) and (B).

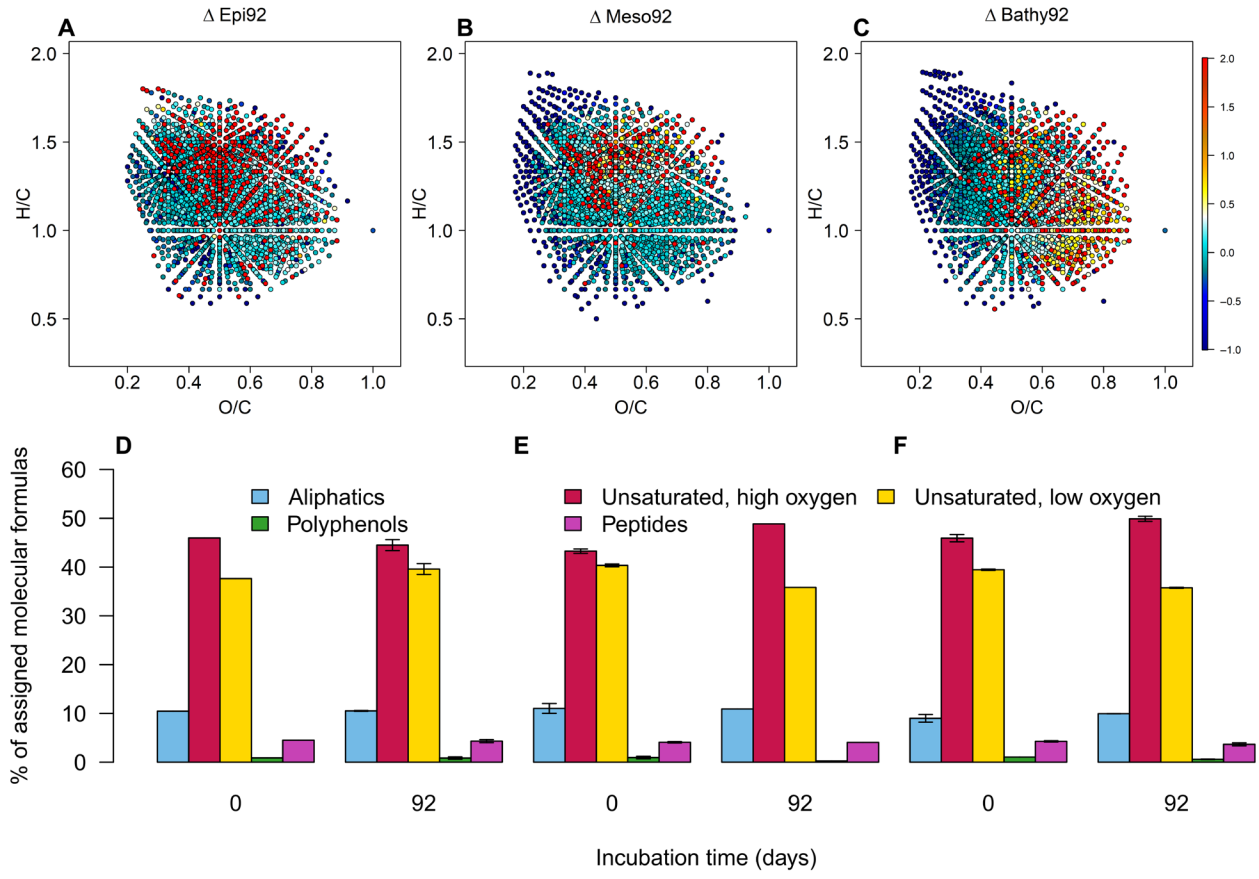

Fig. 2. Changes in DOM composition after 92 days across treatments using ESI-FT-ICR-MS. The top row shows the relative change in the abundance of MF using van Krevelen diagrams comparing MF at 92 days of incubation with those observed at time 0 in the epi- (**A**), meso- (**B**), and bathypelagic (**C**) treatments. Each point represents a MF and is positioned on the basis of its elemental stoichiometry (oxygen:carbon on the *x* axis, hydrogen:carbon on the *y* axis). Cold (dark blue) and hot (yellow to red) colors represent a loss and increase in MF's signal intensity, respectively, and blue-gray color represents marginal signal change over time. The bottom row shows the relative change of groups of compounds comparing MF at 92 days of incubation with those observed at time 0 in the epi- (**D**), meso- (**E**), and bathypelagic (**F**) treatments, where error bars represent the mean absolute deviation between treatment duplicates. Samples were run in negative mode. Each MF was classified on the basis of stoichiometry; polyphenol [0.67 > modified aromaticity index (Almod) > 0.5], unsaturated, low oxygen (Almod < 0.5, H/C < 1.5, O/C < 0.5), unsaturated, high oxygen (Almod < 0.5, H/C < 1.5, O/C ≥ 0.5), aliphatic (H/C ≥ 1.5, N = 0), and peptide-like (H/C ≥ 1.5, N > 0).The two most dynamic groups are unsaturated, low oxygen (yellow, O:C < 0.5) and unsaturated, high oxygen (red, O:C > 0.5) compounds. These results suggest that deeper prokaryotic communities transformed DOM into more refractory compounds as evidenced by the decrease in H:C and increase in O:C caused during the oxidative degradation of DOM, replacing H atoms by O-rich functional groups such as COOH and COH.

Prokaryotic community shifts: Emergence of rare biosphere

Throughout the incubations, the composition of the prokaryotic communities differed substantially between the surface and the deeper meso- and bathy- pelagic treatments, which were found to be more similar (Fig. 3 and fig. S4). In the surface treatment, the four main taxa during the exponential growth were Flavobacteriia (Polaribacter), Alphaproteobacteria (Pelagibacter), a Euryarchaeota (Marine Group II) and a Thaumarchaeota (Nitrosopumilus), representing about 60% of the read abundance, whereas deeper treatments were dominated by Thaumarchaeota and Colwelliaceae, with Rhodobacteraceae appearing later (Fig. 4, A and B). Once total abundance declined (fig. S1), SAR11 remained dominant in the surface treatment, representing up to 60% of the read abundance but was a relatively minor component of the more diverse communities of the deeper treatments (Shannon Index, fig. S5D). However, by combining total abundance using flow cytometry and relative read counts using 16*S*, it appeared that the total abundance of Pelagibacter remained relatively stable at 188 ± 67, 25 ± 25, and 34 ± 36 × 10^3 cells ml^{-1} for the epi-, meso-, and bathypelagic treatments, respectively, for the entire length of the experiment (Fig. 4B).

In all treatments, the prokaryotic communities were highly dynamic showing a succession of rare prokaryotes (Figs. 3 and 4), where most of them were undetectable at the beginning of the incubation (Fig. 4 and fig. S5, A to C). Rare amplicon sequence variants (ASVs) represented between 44 and 86% of the detected ASVs in all treatments but represented a much higher proportion of the abundance in the deep treatments than in the surface (Fig. 4).

DISCUSSION

DOM loss and transformations: Dilution and increased recalcitrance

The MCP framework, as proposed by Jiao *et al.* (*7*), includes two pathways by which prokaryotes create long-lived DOM: the production

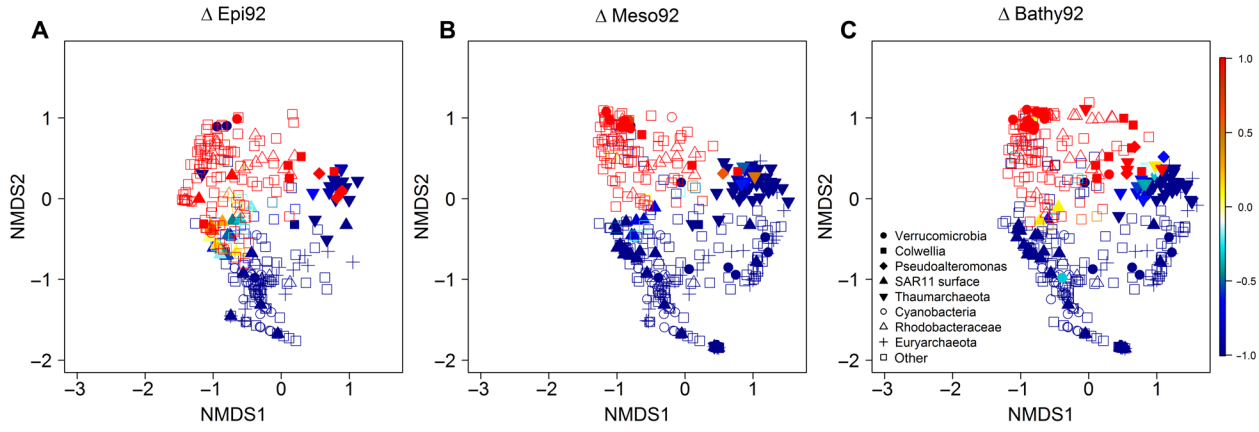

Fig. 3. Prokaryotic community shifts over time among treatments. This figure shows the relative change of amplicon sequence variant (ASV) abundance using a nonmetric multidimensional scaling (NMDS) comparing ASVs at 92 days of incubation with those observed at time 0 in the epi- (**A**), meso- (**B**), and bathypelagic (**C**) treatments. Cold and hot colors represent a decrease and an increase in abundance, respectively. Symbols represent different prokaryotic groups and are the same for each panel. Most of the prokaryotic taxa present after 92 days were not detected at the beginning of the incubation. Successional patterns were similar (fig. S4), but the bathypelagic communities were overall more diverse (fig. S5D). This suggests that a shift in communities is required to consume and transform an increasingly refractory DOM pool. These NMDS were performed using the average abundance of treatment's replicates. The two-dimensional NMDS stress is 0.12.

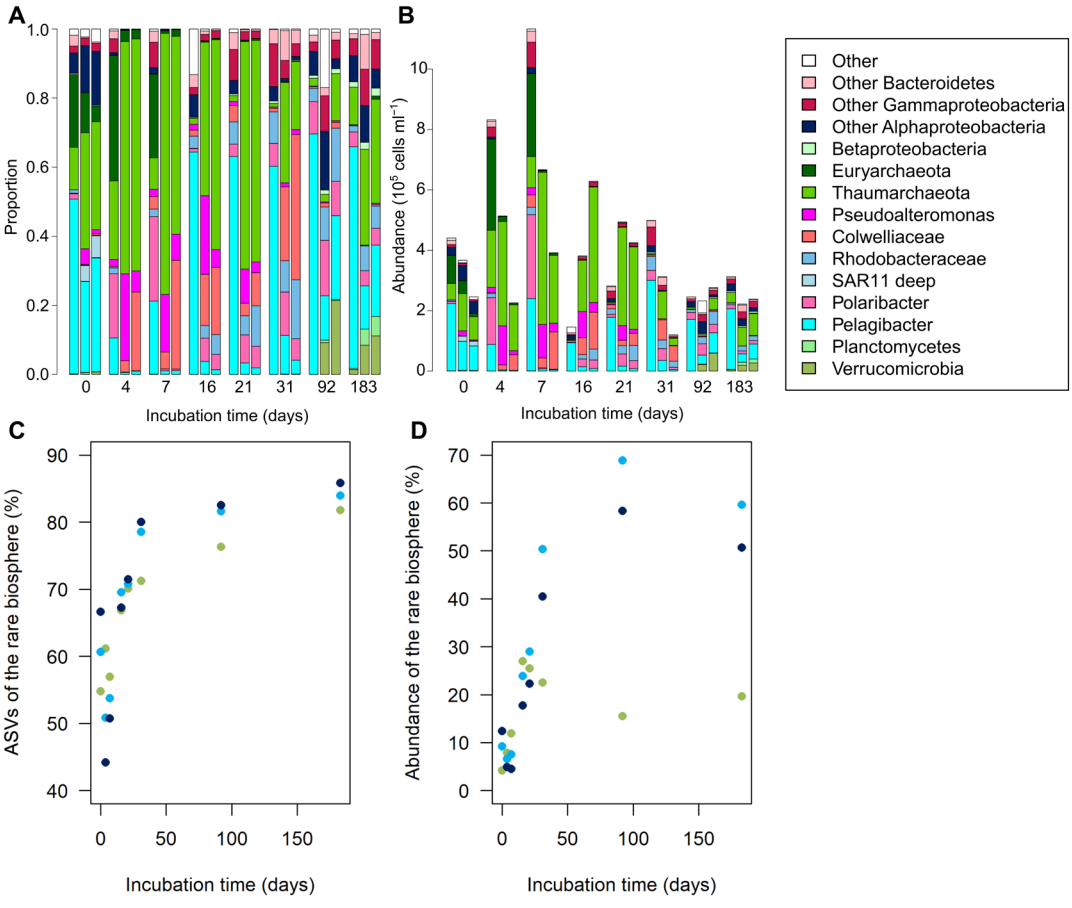

Fig. 4. Time series of the prokaryotic community composition and the rare biosphere. Time series of the prokaryotic community composition expressed as relative (**A**) and total (**B**) abundance and the importance of the rare biosphere, ASV representing less than 0.1% of read abundance, represented as relative richness (**C**) and relative abundance (**D**). We see a rapid response of microbes in the surface treatment where abundance rose rapidly and then crashed, whereas this abundance peak was much less apparent in the deeper treatments. Rare organisms not only represented most of the richness in all treatments but also dominated organism's abundance in the deeper treatments. This suggests that the rare biosphere disproportionately participates in DOM transformation and RDOC production. Green, epipelagic; light blue, mesopelagic; dark blue, bathypelagic.

of intrinsically stable compounds in a given environmental context and the consumption of compounds down to a threshold concentration preventing further uptake (*5*). The dilution hypothesis has also been termed "emergent recalcitrance" (*8*) where RDOC is considered an ecosystem property that emerges from DOM-microbe interactions, similar to the processes that lead to organic carbon preservation in soils (*29*). Metaphorically speaking, ocean storage of RDOC can be compared to carbon stored in peatlands as both sequester carbon for thousands of years (*30*). Accumulated carbon in peat is stored for millennia when peatland sites remain under stable anoxic conditions much like what was suggested in Proterozoic ocean sediments (*14*) but gets rapidly degraded under oxic conditions. Thus, storage is highly context dependent. In the oceans, however, DOM preservation is likely intrinsically stable under various environmental contexts. For instance, up to 16% of old radiocarbon aged DOM from the deep ocean can be incorporated into prokaryotic biomass (*31*). This incorporation can be achieved either through cometabolism with freshly produced DOM, through partial photodegradation (*32*), which can increase DOM lability (*33*), or as a result of fresh DOM with an old radiocarbon signature being consumed (*34*), potentially produced via chemoautotrophy (*35*). Nevertheless, deep ocean DOM persists for thousands of years under oxic conditions and through many ocean circulation cycles. However, a large proportion of oceanic DOM could be labile but too diluted to be energetically profitable for prokaryotes to consume it (*5*). Modeling studies were able to reproduce oceanic DOC profiles by using only diluted compounds (*36*) or a combination of diluted and recalcitrant compounds (*37*). These results thus support the dilution hypothesis as a mechanism for long-term DOC sequestration. However, at most, 5% of DOC was consumed in short-term bioassays of concentrated deep ocean DOM (*6*, *38*), suggesting that dilution represents a minor component of DOC sequestration in the oceans. These findings were also corroborated in another bioassay experiment where seawater was enriched with phytoplankton DOM, concentrated deep ocean DOM extracts, or a combination of both (*10*), where deep ocean DOM showed no sign of further degradation.

Our findings tended to support both the dilution hypothesis and the microbial production of refractory compounds of the MCP. All our treatments, regardless of the inoculum source, reached the same baseline plateau in all treatments of around 50 μM DOC representative of North Atlantic deep ocean (*39*), supporting dilution (*40*). However, during that process, the molecules consumed and produced diverged between the surface and deeper treatments, with the latter producing more recalcitrant compounds. For instance, there was a net loss of unsaturated, low oxygen MF and a net increase of their high oxygen counterparts in both the meso- and bathypelagic treatments (Fig. 2), suggesting increased recalcitrance due to biological degradation (*41*), which was not observed in the surface treatment. We also observed an increase in NOSC of the DOM in the bathypelagic treatment only suggesting the creation of even more recalcitrant compounds compared to the epi- and mesopelagic. High NOSC in DOM probably comes from the partial oxidative degradation of labile DOM leaving behind small molecules with a high proportion of oxygen-containing functional groups (e.g., COOH) such as in CRAM. This is supported by the size-reactivity continuum model (*42*). Oxygenated functional groups, like those found in CRAM, are expected to constitute a strong ligand for metal binding and multiple coordination, promoting aggregation and affecting DOM reactivity (*43*). Moreover, Lechtenfeld *et al.* (*41*) found a positive correlation between NOSC and the compound residence time supporting the idea that the oxygen content of a molecule, at least in part, determines its reactivity.

We observed a slight decrease in CRAM abundance in all treatments, which was not anticipated in the "island of stability" (*41*). This consumption may be related to the composition of the prokaryotic communities, where several taxa (e.g., Euryarchaeota, Thaumarchaeota, and Rhodobacteraceae) observed in all treatments have been recently associated with the degradation of CRAM-like compounds (*44*, *45*). Nevertheless, CRAM relative abundance still represented about 65% of the ultrahigh mass spectrometry signal, and although not all CRAM-like compounds are refractory (*45*), this suggests that most of them have a refractory nature. Although these qualitative changes do not necessarily support production, we observed an increase over time in two fluorescent components, $F_{\lambda em}486$ and $F_{\lambda em}392$, known to be present in the deep ocean (*46*) in all our incubations, providing semiquantitative evidence of production. These two components have a turnover time of 435 and 610 years, respectively (*47*), indicative of their recalcitrance. Our combined results thus confirm the recalcitrance hypothesis of the MCP framework (*3*, *7*, *48*) in all oceanic strata we investigated in the Labrador Sea, but this was most efficient in deeper ocean, where the creation or alteration of more stable DOM molecules contributing to long-term carbon storage in the oceans was evident (Fig. 2).

Prokaryotic community shifts in surface treatment

One of the major differences we observed between the surface versus the deeper meso- and bathypelagic treatments was the high read abundance of Pelagibacter, a taxa that represents about half of all living microbes in the surface ocean (*49*). However, their total abundance in the surface microcosms remained rather constant throughout the incubations, suggesting that they were not particularly active even when more labile substrates were available during the first 2 weeks of the incubation, which resembled bloom conditions at the study site (*50*). This apparent inactivity of Pelagibacter was also observed in other studies (*44*, *50*) and can also explain the slight difference in the relative abundance of the rare biosphere between the two deeper treatments (Fig. 4D) as Pelagibacter accounted for about 10% of the bathypelagic community near the end of the incubation. A more responsive taxa in the surface treatment was Polaribacter whose read abundance followed total cell counts. This agrees with results from the North Sea where Polaribacter preferentially consumed polysaccharides released during natural blooms (*51*). Another responsive taxa was Euryarchaeota, a phylum of archaea generally found in the surface ocean and associated with protein degradation (*52*). This family of compounds is considered labile and therefore should be among the first to be consumed, which is in agreement with the rapid increase and decline of Euryarchaeota in the surface treatment.

Prokaryotic succession with increased DOM recalcitrance in deep treatments

These findings for the surface treatments, however, are in sharp contrast with the dominant taxa in the deeper treatments whose prokaryotic communities were almost entirely composed of taxa belonging to Thaumarchaeota or Colwelliaceae during the first 30 days (Fig. 5). Several Thaumarchaeota are known to be chemoautotrophs oxidizing ammonium to nitrite (*53*), which potentially contribute to labile DOM production in deeper waters (*54*). This production of new

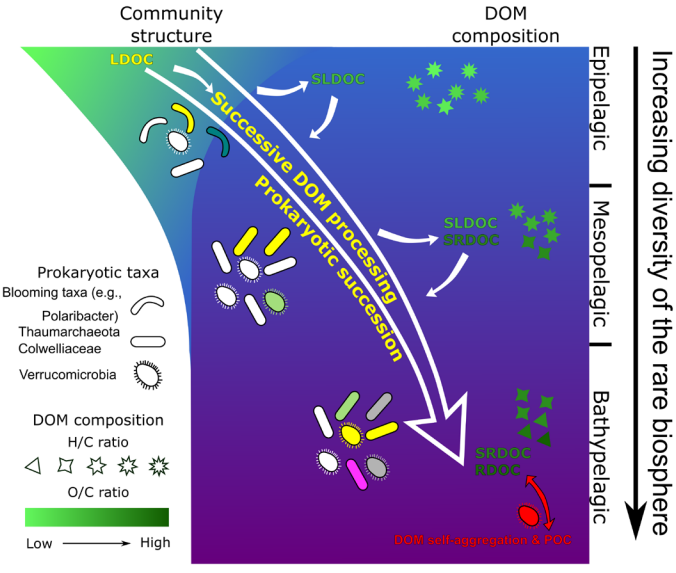

Fig. 5. Conceptual representation of the MCP and DOM-prokaryotic associations. The successive transformation of labile DOM compounds to produce increasingly more RDOC was concomitant to the succession of prokaryotic taxa that was more efficient in deeper communities. Overall, the prokaryotic communities of deep ocean were more diverse after 92 days of incubation as compared to those from the surface and simultaneously produced more recalcitrant compounds, with a lower and higher hydrogen:carbon and oxygen:carbon ratio, respectively. Our results suggest that the bathypelagic was even more efficient than the mesopelagic, but most were not statistically significant. Thaumarchaeota and Colwelliaceae seemed to play an important role in transformation of moderately complex DOM, and Verrucomicrobia became a major member of the community representing 20 to 30% of the abundance as DOM became increasingly recalcitrant over time. Verrucomicrobia are thought to prefer a particle associated lifestyle and, hence, we propose, in red, the formation of particulate organic carbon (POC) through DOM self-aggregation at depth that may increasingly favor C sequestration through the MCP. Our results suggest that not only areas of deep convective mixing such as the Labrador Sea but also mesoscale eddies favor the encounter of DOM and members of the rare biosphere. When such mixing events occur, it potentially creates hotspots of microbial carbon transformations and sequestration. L, labile; SL, semi-labile; SR, semi-refractory; R, refractory. Figure adapted from Jiao *et al.* (*7*).

substrates by Thaumarcheota may help with the cometabolism of more recalcitrant DOM compounds by other microbial heterotrophs in the deeper treatments through priming (*55*). Some Thaumarcheota have also been shown to be mixotrophic (*44*), or even fully heterotrophic (*56*), and likely participate directly in DOM transformation as well. The other taxa, Colwelliaceae, is a family of Gammaproteobacteria known to grow in the deep ocean and is associated with the degradation of moderately complex DOM (*57*). Their high abundance during the first 31 days of the deep experiments suggests that their presence favored the production of RDOC (Fig. 2), which was not observed in the surface treatment. Toward the end of the incubations, 10 to 20 ASVs belonging to Verrucomicrobia, a phylum virtually absent during the earlier portion of the incubations, were detected and abundant after 92 days in the deeper treatments (Fig. 5), suggesting their ability to consume more recalcitrant DOM molecules. There is some evidence that this phylum may be more associated with particles (*58*), which is supported by the higher NOSC in deeper treatments given their potential for aggregation (*43*). A similar prokaryotic succession was reported during long-term incubations of Mediterranean bathypelagic water (*59*), suggesting that the communities responsible for the formation of RDOC as observed in our study likely exist in other deep-sea regions as well.

The deeper treatments were also dominated by members of the rare biosphere. Most of the prokaryotic taxa found after 92 days of incubation were undetectable at the beginning of the experiment, which suggests that taxa from the rare biosphere acted as a "seed bank" (*21*) and contributed to the production of RDOC. Although the successional patterns were similar (fig. S4), prokaryotic communities in deeper treatments were more diverse than those at the surface, and this higher diversity remained throughout much of the incubation (fig. S5D). The observation of higher diversity in the deeper treatments is consistent with the larger genome of deep-sea prokaryotes and their opportunistic lifestyle (*60*). In agreement with succession theory (*61*), our findings support that the rare biosphere possibly harbors a broader metabolic potential to produce a greater variety of DOM compounds.

Mesoscale eddies likely favor MCP more broadly

Deep convective mixing events occurring during winter in the subpolar regions of the ocean are critical for connecting deep prokaryotic communities with DOM from surface layers enabling the RDOC transformation processes observed in this study. Furthermore, deep mesoscales eddies may have a similar effect of mixing differential microbial communities to unseen DOM. Eddies have been shown to contribute to shaping microbial communities and metabolism in the surface ocean (*62*, *63*) and influencing major ocean biogeochemical cycles (*64*). Our results support both phenomena. Samples from our bathypelagic site were taken within a deep energetic (up to ~600 m vertical) mesoscale eddy, which upwelled water from below 1950 m to our sampling depth of 1500 m (see Materials and Methods for details). This likely resulted in the differential rare biosphere observed in our experiments, which created an ecological network (*8*) unseen in the surface treatment, hence creating more increasingly stable DOM compounds. Hence, our findings may have broader implications on DOM cycling because mixing of water masses by mesoscale eddies is a common ocean feature both in surface and deep waters (*27*). Eddies increase the probability that unique prokaryotic communities encounter substrates from different water masses for which they harbor the right enzymes (*8*, *65*) to mineralize it to CO_2 (*32*) or convert a fraction of the bulk DOC into RDOC.

Experimental limitations

Although bottle incubations have limitations (*66*), they serve to test natural phenomena that would otherwise be practically impossible (*67*). Here, we sought to emulate a mixing event of winter overturn that in situ takes a few weeks to occur within the region (*68*); hence, the immediate injection of deep microbes to filtered surface waters does not take into account the DOM that is transformed during the convective process. Bottle experiments also modify the immediate environments of microbes and can induce a selection pressure for taxa that better tolerate these conditions. For example, the metabolic wastes and metabolites of microbes are contained within the bottles whereas they would tend to be diluted in nature. However, the DOM transformations observed in vitro also likely occur in nature as the metabolic wastes and metabolites would be similar. Hence, the main result that deeper prokaryotic communities produce stable molecules through subsequent transformations is supported and

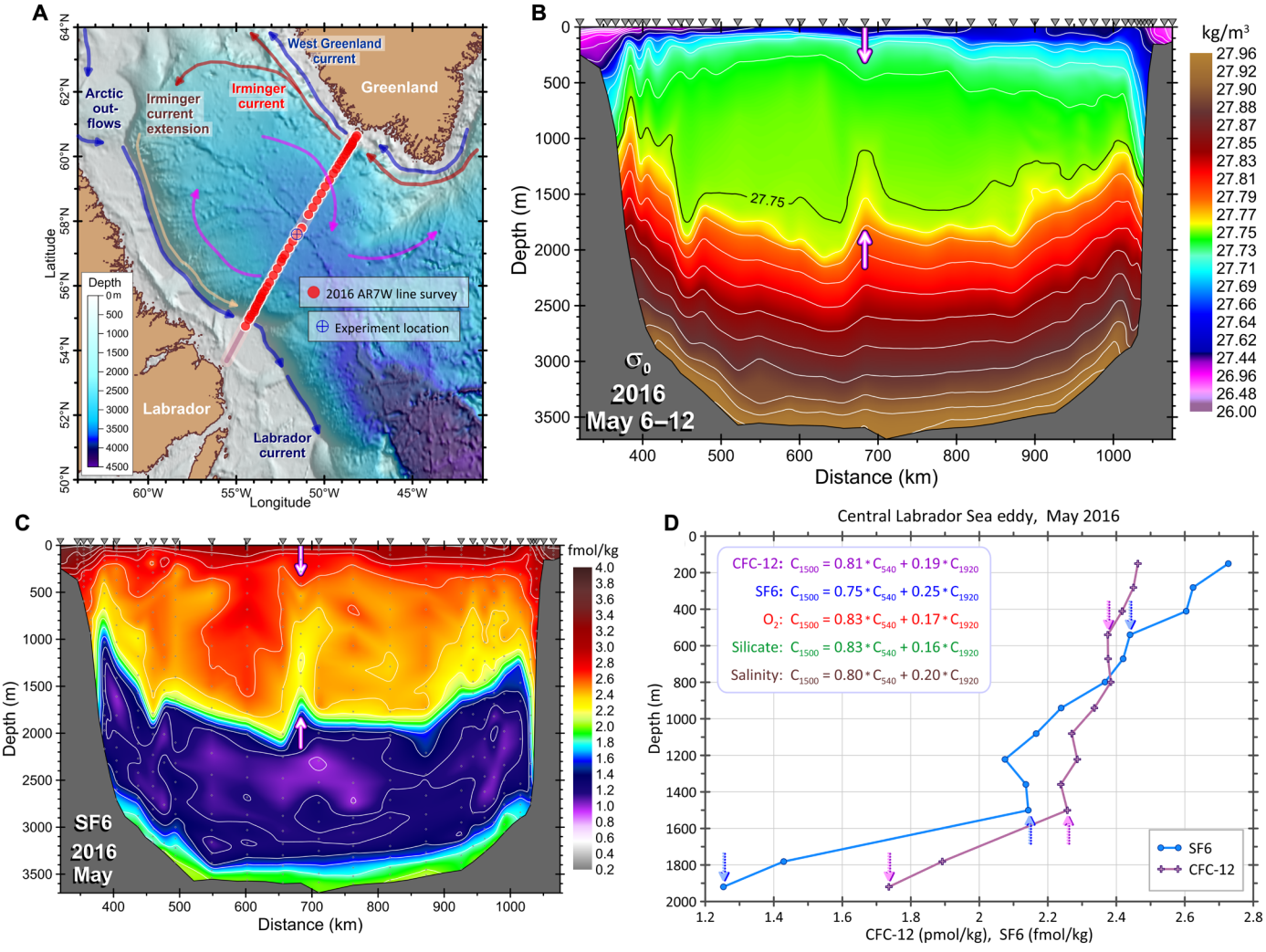

Fig. 6. Map, cross sections, and profiles of water masses tracers in the Labrador Sea. Topography, major upper-ocean circulation features (red arrows indicate waters of subtropical origin and blue arrows indicates waters of subpolar origin) and the repeat oceanography line AR7W in the Labrador Sea in May of 2016 (**A**). The oceanographic stations occupied in May of 2016 onboard CCGS Hudson are indicated (red dots), and the sampling site (blue crossed circle) was chosen for this experiment. Cross section of density (**B**) and SF6 (fmol/kg, **C**) that shows the mesoscale eddy located in the middle of the AR7W transect. The cyclonic (counterclockwise spinning) eddy mentioned in the text is associated with upward displacement of density contours in the middle of the line. Vertical profiles of CFC-12 (nmol/kg) and SF6 (fmol/kg) (**D**). The equations included in (C) represent mixing ratios containing the fractions of LSW_{2016} and deeper water required to produce the water mass sampled at 1500 m based on the water sample values indicated with the arrows. As mesoscale eddies are common physical features in the global ocean (*25*), our results are likely transposable to other mesoscale eddies as different water masses mix together. Here, the mesoscale eddy brought about 20% of deeper water to our sampling depth, thus creating opportunities for DOM and microbes to encounter. See Groeskamp *et al.* (*92*) for a global map of eddies diffusivity.

would be difficult to prove otherwise. The other main limitation of our study is the use of only duplicates due to space and water limitations and the various arrays of methods used. Although DOC, FDOM, FT-ICR-MS, and 16*S* results suggest that bathypelagic communities were more efficient at degrading organic carbon and producing stable molecules, few results were statistically different from the mesopelagic treatment in large part due to our low statistical power. Nevertheless, our results indicate that deeper ocean prokaryotes transform DOM differently than their surface counterparts and likely produce compounds that are more persistent.

Our study confirms the production of intrinsically more recalcitrant DOM molecules in natural waters via the MCP. Similar to other studies, our work shows that DOM production can be stimulated by communities from different oceanic strata with the iterative production of more refractory compounds through prokaryotic community succession (*69*) with taxa emerging from the rare biosphere (Fig. 5). Moreover, our work also supports the concentration limited recalcitrance hypothesis where we found that regardless of the prokaryotic community composition, all treatments converged to the same final bulk DOC concentration, reflecting that of the deep ocean at our study site, however, with different MF signatures. Deeper prokaryotic communities, which were found to be more diverse in their successional response than the surface ones, were clearly more efficient at producing RDOC. Hence, our findings suggest that deep water formation sites such as the Labrador Sea could be hotspots in the global ocean in carbon sequestration through the MCP because

of their unusually deep convective mixing. Furthermore, there is potentially a higher sequestration in years when winter convection reaches the bathypelagic zone as compared to shallower mixing years. We confirm that communities in deeper strata were more diverse in their rare biosphere, which supports greater metabolic potential for recalcitrant DOM production further facilitating long-term carbon sequestration in the ocean through the MCP.

MATERIALS AND METHODS

Study site, water mass, and deep eddy characterization

Samples were collected in the Labrador Sea on 14 May 2016 near its central location (57.59°N, 51.57°W) on the Atlantic Repeat Hydrography Line 7 West (Fig. 6A). The site and depths that we sampled were specifically chosen to capture the influence of a deep mesoscale eddy (Fig. 6B), which contrasted with other locations that mainly containing the new, nearly homogeneous Labrador Sea Water (LSW; fig. S6A). Pressure, temperature (SBE35), salinity, and dissolved oxygen (SBE43) data from the conductivity-temperature-depth (CTD) were quality-controlled and calibrated to meet World Ocean Circulation Experiment standards using water samples. Salinity was measured on an Autosal salinometer, and dissolved oxygen concentration was measured using a Winkler titration system. Silicate was kept frozen at 20°C until onboard analysis using an Alpkem RFA-300 autoanalyzer.

SF6 and CFC-12 profiles were also conducted (Fig. 6). Samples of both gases were drawn directly from Niskin bottles into 250-ml glass syringes, stored at 2°C for a maximum of 12 hours, and then warmed to 20°C before analysis on a custom-made purge-and-trap system where dissolved gases were stripped from the sample in a stream of ultrahigh purity nitrogen. Both gases were quantitatively retained in a trap comprising 30 cm of 1/16″ stainless steel tubing packed with 100- to 120-mesh Carboxen 1000 held at −70°C. After each 7-min purge cycle, the trap was heated to 180°C, and the desorbed gases were directed to a Varian gas chromatograph equipped with an electron-capture detector. SF6 and CFC-12 were separated on a 1-m precolumn packed with Porasil B and a 2-m main column packed with Molecular Sieve 5A held at 80°C. The chromatographic sample peaks were quantified with Varian Galaxie software, and the analytical system was calibrated at least once each day using an air standard supplied by CMDL/NOAA, Boulder, Colorado. Analytical precision as determined by repeated standard injections was ±5% for SF6 and ±1% for CFC-12.

The two anthropogenic gases, SF6 and CFC-12, are commonly used as tracers for convectively formed and therefore well-ventilated water masses. The most recently ventilated version of LSW at time of the survey was LSW_{2016}. It was formed in the previous winter and can be easily identified in the section plots (Fig. 6 and fig. S6) as a well-mixed homogenized layer extending from a few hundreds to 2000 m. LSW_{2016} is part of the 2012–2018 LSW class (*24*), progressively formed during the winters of 2012 to 2015. Vertical profiles of salinity, dissolved oxygen, silicate, SF6, and CFC-12 concentrations, supported by time series of salinity at different depths obtained from profiling Argo float data, were used to calculate the mixing ratios at 540 and 1500 m with surface water and deeper water, respectively.

To confirm the influence of the deep convective eddy on creating distinctive microbial communities in the Labrador Sea, we calculated the mixing ratio for the meso- and bathypelagic depths we sampled. On the basis of the seasonal progression in salinity, we estimated that the mesopelagic water was composed of 10% of surface water to bring down the salinity from 34.86 to 34.81 from late autumn to after the winter convective mixing in April (fig. S6B). In contrast, the five different tracers (salinity, oxygen, silicate, CFC-12, and SF6; Fig. 6) suggest that the bathypelagic water was composed of 81 ± 4% from LSW_{2016} and 19 ± 4% of water upwelled from a deeper stratum, confirming that our three experimental treatments were inoculated with three different water masses and hence distinct microbial communities.

Microcosm preparation

Epipelagic water was sampled at 20 m, mesopelagic at 540 m, and bathypelagic at 1500 m on the upward CTD cast. Water was collected and filtered through 53-μm mesh into acid-washed high-density polyethylene carboys and transported to the laboratory immediately for processing. Epipelagic water was consecutively filtered through a 3-μm polycarbonate filter and a 0.2-μm polyethersulfone filter using a peristaltic system equipped with silicone tubing. The filtrate (medium) was homogenized in an acid-washed polyethylene carboy. Time series incubations were carried out in 11 liters of acid and base-washed glass carboys with silicone stoppers ("microcosm") in duplicates. Each microcosm received 8 liters of epipelagic 0.2-μm filtered medium and a 2-liter inoculum 53-μm filtered source water collected from epi-, meso-, or bathypelagic depths, representing the three different treatments that were tested. We considered our surface treatment to be our control as we used it as a point of comparison with the meso- and bathypelagic treatments.

Microcosms were kept in the dark at 4°C during the entire experiment to emulate natural conditions and sampled several times for the first 3 months and after 1.5 years. To avoid contamination, 1-liter samples were collected from each microcosm into an acid-washed, preconditioned glass bottle and then subsampled using a nano-pure water-rinsed, preconditioned 60-ml glass syringe with silicone tubing for DOM and prokaryotic characterization. Measurements were chosen to describe specific components of DOM-microbe interactions (*50*). Although DOM and DOC are often used interchangeably, we used DOC when specifically referring to carbon and to DOM otherwise.

DOM characterization

DOC subsamples were acidified at pH < 2 using 12 M HCl (Thermo Fisher Scientific, ACS Plus) and stored in precombusted (450°C for 5 hours) amber glass vials. Since incubation water was prefiltered, DOC subsamples were measured directly and may contain negligible amounts of POC. DOC was measured using high-temperature catalytic oxidation method on an Aurora 1030C mounted with a GD-100 CO_2 trap (*70*) or a Shimadzu TOC-L/TN-TMNL analyzer, with a detection limit of 0.4 μmol C $liter^{-1}$ and 2 to 3 μmol C $liter^{-1}$, respectively. All DOC results were validated against homemade standards or Hansell's consensus reference material (deep seawater reference) (*71*).

Changes in the DOM pool were characterized using ESI-FT-ICR-MS. Water was sequentially filtered through a 3-μm polycarbonate filter and a 0.2-μm polyethersulfone filter with a peristaltic pump using acid-washed silicone tubing. Water samples were then acidified to pH < 2 using 12 M HCl and frozen until extraction. Extractions were performed using Bond Elut PPL cartridges (100 mg; Agilent) (*72*), and volumes were adjusted on the basis of DOC concentrations to extract the same carbon quantity, assuming a 40% DOC

recovery. PPL cartridges were dried using pure N_2 gas, and DOM was recovered using methanol (high-performance liquid chromatography grade). Samples were injected into a 9.4-T ESI-FT-ICR-MS at the National High Magnetic Field Laboratory (Tallahassee, FL) (*73*). Peaks were picked at 6 SD of the root mean square baseline noise, and formula assignment was performed using an in-house protocol (EnviroOrg) (*74*) within these limits: $C_{1–45}H_{1–92}N_{0–4}O_{1–25}S_{0–2}$. To standardize all samples to an equivalent noise threshold, we normalized the numbers of assigned peaks as follows: (i) $f(x) = 0$ if $x < threshold$; (ii) $f(x) = x$ if $x \geq$ Threshold, and (iii) $f(x) = x \times 10{,}000$/sum of sample signal, where x is the intensity signal and Threshold is the second worst noise signal. We focused on the 0- to 92-day samples as they were analyzed within a few days, whereas those of 183 days of incubation were analyzed several months later.

We summarized FT-ICR-MS data to easily look at changes in MF over time and among treatments by calculating relative change in MF as follows: (sample 1 − sample 2)/sample 2. We represented the results in van Krevelen spaces by color coding MF based on the relative change. In cases where no MF were detected in sample 2 but were in sample 1, we modified the relative change to 1. We also present different aspects of DOM composition. We calculated the average O/C ratio of all MF using their respective O/C ratio and their relative abundance at a given time for both treatment replicates. Each MF was classified on the basis of stoichiometry; polyphenol [0.67 > modified aromaticity index (AImod) > 0.5], unsaturated, low oxygen (AImod < 0.5, H/C < 1.5, O/C < 0.5), unsaturated, high oxygen (AImod < 0.5, H/C < 1.5, O/C ≥ 0.5), aliphatic (H/C ≥ 1.5, N = 0), and peptide-like (H/C ≥ 1.5, N > 0) (*75*–*77*). We did the same with NOSC (*78*) and with CRAM following Hertkorn *et al.* (*43*) classification using double bond equivalent (DBE): DBE/C = 0.30 to 0.38, DBE/H = 0.20 to 0.95, and DBE/O = 0.77 to 1.75. Reproducibility of data acquired by ESI ultrahigh-resolution MS for individual samples on multiple different instrument platforms is reported in detail by Hawkes *et al.* (*79*). Although ESI-FT-ICR-MS data are not quantitative and therefore cannot unequivocally confirm an increase or decrease in compound abundance, it can provide semiquantitative information by measuring relative changes in signal magnitude (relative abundance). The solid-phase extractions of DOM required to perform FT-ICR-MS selectively isolate more refractory components, whereas more labile molecules such as carbohydrates and amino acids are not well recovered. Hence, early shifts in microbial communities cannot be easily related to FT-ICR-MS data because of the mismatch between what was consumed by microbes and what was captured with the mass spectrometer. However, we focused our interpretation of mass spectrometry data to later during the incubations where such labile compounds are likely exhausted (*80*) to limit the extent of this bias.

FDOM was measured on a Cary Eclipse spectrofluorometer on 0.2-μm filtered water, with both excitation and emission slit widths of 5 nm. Excitation emission matrices (EEM) were produced by repeatedly scanning over even emission wavelengths between 230 and 600 nm for each excitation wavelength between 220 and 450 nm with a 5-nm excitation increment. Standard corrections were applied to each EEM using the paRafac.correction R library (*81*) except for the inner filter effect as absorbance values were below 0.3 cm^{-1} (*82*). The parallel factor analysis (PARAFAC) model was done with 56 samples using the drEEM (v0.1.0) MATLAB toolbox (*83*). Four independent fluorescent components were validated by split half and random initialization parameters.

Prokaryotic characterization

Prokaryotic community composition was estimated using the 16*S* ribosomal RNA (rRNA) gene. Filters from ESI-FT-ICR-MS filtrations were recovered for DNA analysis and conserved in lysis buffer (40 mM EDTA, 50 mM tris, and 750 mM sucrose), flash-frozen, and stored at −80°C until further processing. DNA was extracted using Qiagen DNeasy Power Water and quantified using a Qubit 2.0 fluorometer high-sensitivity kit, following the manufacturers' instructions. DNA amplification, library preparation, and Illumina sequencing of 16*S* rRNA genes were done at the Integrated Microbiome Resources at Dalhousie University (*84*). A dual-indexing, one-step polymerase chain reaction (PCR) was done using a Nextera XT v2 kit (Illumina) with the adapters and index provided by the kit. Region V6-V8, 16*S* rRNA gene for bacteria was targeted with primers B969F (ACGCGHNRAACCTTACC) and BA1406R (ACGGGCRGTGWGTRCAA) and for Archaea with A956F (TYAATYGGANTCAACRCC) and A1401R (CRGTGWGTRCAAGGRGCA) (*85*). PCR amplification was run for 30 cycles. The amplicon quality was visualized with a 96-well E-gel (Invitrogen), purified and normalized with the high-throughput SequalPrep 96-well Plate Kit (Invitrogen). Samples were pooled to make one library and quantified using Qubit double-stranded DNA high-sensitivity kit (Invitrogen).

Reads were analyzed with the DADA2 pipeline following the tutorial v.1.14 (*86*) using the R software v.3.6.2. After the processing, 2290 ASVs (2,048,513 reads) were obtained for bacterial sequencing and 330 ASV (695,993 reads) for archaea. These were then taxonomically classified on the basis of the SILVA database v132. Archaea were removed from the bacterial dataset, and bacteria were removed from the archaeal dataset to avoid duplication; datasets were then combined for a total of 2504 ASVs.

We corrected the number of sequences with the average number of 16*S* gene copies for each ASV using information provided on the rrnDB website (https://rrndb.umms.med.umich.edu, February 2020). The number of gene copies ranged from 1 to 21, with an overall mean of 3.5 ± 2.2 (SD). When the 16*S* copy number was not found at the genus level, we took the average 16*S* copy of the next taxonomic rank until all ASV abundances were corrected. This resulted in 21.6% of all ASVs corrected at the genus level, and this proportion increased to 75.3% at the order level. All ASVs with a number of reads equal to or less than 10 in a single sample were treated as noise and removed. After all corrections were made, the final ASV count was 1063. A schematic of all steps involved is presented in fig. S7.

The Shannon diversity index was calculated on the whole community and on two different phyla. Briefly, we transformed abundance data into relative abundance and then extracted these for Verrucomicrobia and Thaumarchaeota to calculate their contribution to the overall diversity. Raw reads were deposited on National Center for Biotechnology Information (PRJNA598915), and a summary file containing all taxonomic gene copy information is available at www.github.com/LaboMaranger/MCP.

We measured prokaryotic heterotrophic production over time following Smith and Azam (*87*). Triplicate 1.5-ml samples with a trichloroacetic acid (TCA)–killed control were incubated at in situ temperature in the dark with [3,4,5-^{3}H]-L-leucine (~10 nM final concentration) for 3 hours. Incubations were stopped by adding TCA (5% final), vortexed, centrifuged at 17,000*g* using an accuSpin micro17 centrifuge and siphoned to the last drop. Vials filled with scintillation cocktail were read on a Tri-carb 2800TR scintillation

counter. For rates, a conversion factor of 1550 g C mol leucine^{-1} was used (*88*).

Prokaryotic abundance was counted using flow cytometry. Samples were fixed with 0.1% final concentration glutaraldehyde grade I, flash-frozen, and kept at −80°C until analysis. Thawed samples were stained with SYBR green 1 (1% final concentration) in tris-EDTA buffer (10 mM tris and 1 mM EDTA) (*89*) for 10 min in the dark and counted on a BD Accuri C6 flow cytometer. Specific production was calculated as the ratio of biomass production over cell abundance.

Statistical analysis

DOC decay curves were modeled with a two-pool multi-G approach using a Levenberg-Marquardt optimization to estimate the time required to reach baseline as described in (*80*). The model output gives the decay constant (k) associated to the metabolizable pool along with the proportion of both bioavailable (BDOC) and constant pool (RDOC). The optimization iteratively fits a curve to these points by changing all parameters at once where the best model was chosen on the basis of the lowest residuals of the sum of squares. The time required to reach the plateau can be estimated as such: $1/k \times 5$ (*80*).

To represent how communities shifted during the experiment, we conducted a two-dimensional nonmetric multidimensional scaling (NMDS) (*90*) based on Bray-Curtis transformed data. To show how the prokaryotic community changed over time among treatments, relative changes in ASV abundance were determined as described for MF in the ESI-FT-ICR-MS. A third axis reduced the overall stress from 0.12 to 0.06 but did not change the interpretation. All statistics were done using R v3.6.2 (*91*).

SUPPLEMENTARY MATERIALS

Supplementary material for this article is available at https://science.org/doi/10.1126/sciadv.abn0035

REFERENCES AND NOTES

1. D. A. Hansell, C. A. Carlson, D. J. Repeta, R. Schlitzer, Dissolved organic matter in the ocean: A controversy stimulates new insights. *Oceanography* **22**, 202–211 (2009).
2. A. B. A. Daoud, L. Tremblay, HPLC-SEC-FTIR characterization of the dissolved organic matter produced by the microbial carbon pump. *Mar. Chem.* **215**, 103668 (2019).
3. H. Ogawa, Y. Amagai, I. Koike, K. Kaiser, R. Benner, Production of refractory dissolved organic matter by bacteria. *Science* **292**, 917–920 (2001).
4. N. Jiao, G. J. Herndl, D. A. Hansell, R. Benner, G. Kattner, S. W. Wilhelm, D. L. Kirchman, M. G. Weinbauer, T. Luo, F. Chen, F. Azam, Microbial production of recalcitrant dissolved organic matter: Long-term carbon storage in the global ocean. *Nat. Rev. Microbiol.* **8**, 593–599 (2010).
5. D. E. LaRowe, A. W. Dale, J. P. Amend, P. Van Cappellen, Thermodynamic limitations on microbially catalyzed reaction rates. *Geochim. Cosmochim. Acta* **90**, 96–109 (2012).
6. J. M. Arrieta, E. Mayol, R. L. Hansman, G. J. Herndl, T. Dittmar, C. M. Duarte, Dilution limits dissolved organic carbon utilization in the deep ocean. *Science* **348**, 331–333 (2015).
7. N. Jiao, C. Robinson, F. Azam, H. Thomas, F. Baltar, H. Dang, N. Hardman-Mountford, M. Johnson, D. Kirchman, B. Koch, L. Legendre, C. Li, J. Liu, T. Luo, Y.-W. Luo, A. Mitra, A. Romanou, K. Tang, X. Wang, C. Zhang, R. Zhang, Mechanisms of microbial carbon sequestration in the ocean–future research directions. *Biogeosciences* **11**, 5285–5306 (2014).
8. T. Dittmar, S. T. Lennartz, H. Buck-Wiese, D. A. Hansell, C. Santinelli, C. Vanni, B. Blasius, J.-H. Hehemann, Enigmatic persistence of dissolved organic matter in the ocean. *Nat. Rev. Earth Environ.* **2**, 570–583 (2021).
9. L. Legendre, R. B. Rivkin, M. G. Weinbauer, L. Guidi, J. Uitz, The microbial carbon pump concept: Potential biogeochemical significance in the globally changing ocean. *Prog. Oceanogr.* **134**, 432–450 (2015).
10. Y. Shen, R. Benner, Molecular properties are a primary control on the microbial utilization of dissolved organic matter in the ocean. *Limnol. Oceanogr.* **65**, 1061–1071 (2020).
11. K. Kaiser, R. Benner, Major bacterial contribution to the ocean reservoir of detrital organic carbon and nitrogen. *Limnol. Oceanogr.* **53**, 99–112 (2008).
12. R. Benner, K. Kaiser, Abundance of amino sugars and peptidoglycan in marine particulate and dissolved organic matter. *Limnol. Oceanogr.* **48**, 118–128 (2003).
13. M. D. McCarthy, J. I. Hedges, R. Benner, Major bacterial contribution to marine dissolved organic nitrogen. *Science* **281**, 231–234 (1998).
14. G. A. Logan, J. M. Hayes, G. B. Hieshima, R. E. Summons, Terminal Proterozoic reorganization of biogeochemical cycles. *Nature* **376**, 53–56 (1995).
15. B. P. Koch, G. Kattner, M. Witt, U. Passow, Molecular insights into the microbial formation of marine dissolved organic matter: Recalcitrant or labile? *Biogeosciences* **11**, 4173–4190 (2014).
16. J. A. Fuhrman, Å. Hagström, Bacterial and archaeal community structure and its patterns, in *Microbial Ecology of the Oceans* (Wiley, ed. 2, 2008), pp. 45–90.
17. M. T. Cottrell, D. L. Kirchman, Natural assemblages of marine proteobacteria and members of the Cytophaga-Flavobacter cluster consuming low-and high-molecular-weight dissolved organic matter. *Appl. Environ. Microbiol.* **66**, 1692–1697 (2000).
18. M. Mestre, C. Ruiz-González, R. Logares, C. M. Duarte, J. M. Gasol, M. M. Sala, Sinking particles promote vertical connectivity in the ocean microbiome. *Proc. Natl. Acad. Sci.* **115**, E6799–E6807 (2018).
19. M. L. Sogin, H. G. Morrison, J. A. Huber, D. M. Welch, S. M. Huse, P. R. Neal, J. M. Arrieta, G. J. Herndl, Microbial diversity in the deep sea and the underexplored "rare biosphere". *Proc. Natl. Acad. Sci.* **103**, 12115–12120 (2006).
20. M. D. J. Lynch, J. D. Neufeld, Ecology and exploration of the rare biosphere. *Nat. Rev. Microbiol.* **13**, 217–229 (2015).
21. J. T. Lennon, S. E. Jones, Microbial seed banks: The ecological and evolutionary implications of dormancy. *Nat. Rev. Microbiol.* **9**, 119–130 (2011).
22. T. M. Lenton, H. Held, E. Kriegler, J. W. Hall, W. Lucht, S. Rahmstorf, H. J. Schellnhuber, Tipping elements in the Earth's climate system. *Proc. Natl. Acad. Sci. U.S.A.* **105**, 1786–1793 (2008).
23. M. D. DeGrandpre, A. Kortzinger, U. Send, D. W. R. Wallace, R. G. J. Bellerby, Uptake and sequestration of atmospheric CO_2 in the Labrador Sea deep convection region. *Geophys. Res. Lett.* **33**, 5 (2006).
24. I. Yashayaev, J. W. Loder, Recurrent replenishment of Labrador Sea Water and associated decadal-scale variability. *J. Geophys. Res. Oceans* **121**, 8095–8114 (2016).
25. C. A. Carlson, S. J. Giovannoni, D. A. Hansell, S. J. Goldberg, R. Parsons, K. Vergin, Interactions among dissolved organic carbon, microbial processes, and community structure in the mesopelagic zone of the northwestern Sargasso Sea. *Limnol. Oceanogr.* **49**, 1073–1083 (2004).
26. I. Yashayaev, J. W. Loder, Further intensification of deep convection in the Labrador Sea in 2016. *Geophys. Res. Lett.* **44**, 1429–1438 (2017).
27. P. B. Rhines, *Mesoscale Eddies*, S. J. H. Ed. (Encyclopedia of ocean sciences, Academic Press, 2001).
28. C. A. Carlson, H. W. Ducklow, Growth of bacterioplankton and consumption of dissolved organic carbon in the Sargasso Sea. *Aquat. Microb. Ecol.* **10**, 69–85 (1996).
29. M. W. Schmidt, M. S. Torn, S. Abiven, T. Dittmar, G. Guggenberger, I. A. Janssens, M. Kleber, I. Kögel-Knabner, J. Lehmann, D. A. Manning, Persistence of soil organic matter as an ecosystem property. *Nature* **478**, 49–56 (2011).
30. P. M. Williams, E. R. M. Druffel, Radiocarbon in dissolved organic matter in the central North Pacific Ocean. *Nature* **330**, 246–248 (1987).
31. J. Cherrier, J. E. Bauer, E. R. M. Druffel, R. B. Coffin, J. P. Chanton, Radiocarbon in marine bacteria: Evidence for the ages of assimilated carbon. *Limnol. Oceanogr.* **44**, 730–736 (1999).
32. Y. Shen, R. Benner, Mixing it up in the ocean carbon cycle and the removal of refractory dissolved organic carbon. *Sci. Rep.* **8**, 1–9 (2018).
33. D. J. Kieber, J. McDaniel, K. Mopper, Photochemical source of biological substrates in sea water: Implications for carbon cycling. *Nature* **341**, 637–639 (1989).
34. C. L. Follett, D. J. Repeta, D. H. Rothman, L. Xu, C. Santinelli, Hidden cycle of dissolved organic carbon in the deep ocean. *Proc. Natl. Acad. Sci. U.S.A.* **111**, 16706–16711 (2014).
35. C. Berg, L. Listmann, V. Vandieken, A. Vogts, K. Jürgens, Chemoautotrophic growth of ammonia-oxidizing Thaumarchaeota enriched from a pelagic redox gradient in the Baltic Sea. *Front. Microbiol.* **5**, 786 (2015).
36. A. Mentges, C. Feenders, C. Deutsch, B. Blasius, T. Dittmar, Long-term stability of marine dissolved organic carbon emerges from a neutral network of compounds and microbes. *Sci. Rep.* **9**, 1–13 (2019).
37. E. J. Zakem, B. B. Cael, N. M. Levine, A unified theory for organic matter accumulation. *Proc. Natl. Acad. Sci.* **118**, e2016896118 (2021).
38. N. Wang, Y. W. Luo, L. Polimene, R. Zhang, Q. Zheng, R. Cai, N. Jiao, Contribution of structural recalcitrance to the formation of the deep oceanic dissolved organic carbon reservoir. *Environ. Microbiol. Rep.* **10**, 711–717 (2018).
39. D. A. Hansell, Recalcitrant dissolved organic carbon fractions. *Ann. Rev. Mar. Sci.* **5**, 421–445 (2013).
40. J. J. Middelburg, Escape by dilution. *Science* **348**, 290–290 (2015).
41. O. J. Lechtenfeld, G. Kattner, R. Flerus, S. L. McCallister, P. Schmitt-Kopplin, B. P. Koch, Molecular transformation and degradation of refractory dissolved organic matter in the Atlantic and Southern Ocean. *Geochim. Cosmochim. Acta* **126**, 321–337 (2014).

42. R. Benner, R. M. Amon, The size-reactivity continuum of major bioelements in the ocean. *Ann. Rev. Mar. Sci.* **7**, 185–205 (2015).
43. N. Hertkorn, R. Benner, M. Frommberger, P. Schmitt-Kopplin, M. Witt, K. Kaiser, A. Kettrup, J. I. Hedges, Characterization of a major refractory component of marine dissolved organic matter. *Geochim. Cosmochim. Acta* **70**, 2990–3010 (2006).
44. N. McDonald, E. P. Achterberg, C. A. Carlson, M. Gledhill, S. Liu, J. R. Matheson-Barker, N. B. Nelson, R. J. Parsons, The role of heterotrophic bacteria and archaea in the transformation of lignin in the open ocean. *Front. Mar. Sci.* **6**, (2019).
45. S. Liu, R. Parsons, K. Opalk, N. Baetge, S. Giovannoni, L. M. Bolaños, E. B. Kujawinski, K. Longnecker, Y. Lu, E. Halewood, C. A. Carlson, Different carboxyl-rich alicyclic molecules proxy compounds select distinct bacterioplankton for oxidation of dissolved organic matter in the mesopelagic Sargasso Sea. *Limnol. Oceanogr.* **65**, 1532–1553 (2020).
46. Y. Yamashita, R. M. Cory, J. Nishioka, K. Kuma, E. Tanoue, R. Jaffé, Fluorescence characteristics of dissolved organic matter in the deep waters of the Okhotsk Sea and the northwestern North Pacific Ocean. *Deep-Sea Res. II Top. Stud. Oceanogr.* **57**, 1478–1485 (2010).
47. T. S. Catalá, I. Reche, A. Fuentes-Lema, C. Romera-Castillo, M. Nieto-Cid, E. Ortega-Retuerta, E. Calvo, M. Álvarez, C. Marrasé, C. A. Stedmon, X. A. Álvarez-Salgado, Turnover time of fluorescent dissolved organic matter in the dark global ocean. *Nat. Commun.* **6**, 5986 (2015).
48. R. T. Barber, Dissolved organic carbon from deep waters resists microbial oxidation. *Nature* **220**, 274–275 (1968).
49. S. J. Giovannoni, SAR11 bacteria: The most abundant plankton in the oceans. *Ann. Rev. Mar. Sci.* **9**, 231–255 (2017).
50. R. LaBrie, S. Bélanger, R. Benner, R. Maranger, Spatial abundance distribution of prokaryotes is associated with dissolved organic matter composition and ecosystem function. *Limnol. Oceanogr.* **66**, 575–587 (2020).
51. P. Xing, R. L. Hahnke, F. Unfried, S. Markert, S. Huang, T. Barbeyron, J. Harder, D. Becher, T. Schweder, F. O. Glöckner, R. I. Amann, H. Teeling, Niches of two polysaccharide-degrading Polaribacter isolates from the North Sea during a spring diatom bloom. *ISME J.* **9**, 1410–1422 (2015).
52. L. H. Orellana, T. Ben Francis, K. Krüger, H. Teeling, M.-C. Müller, B. M. Fuchs, K. T. Konstantinidis, R. I. Amann, Niche differentiation among annually recurrent coastal Marine Group II Euryarchaeota. *ISME J.* **13**, 3024–3036 (2019).
53. M. Könneke, A. E. Bernhard, R. José, C. B. Walker, J. B. Waterbury, D. A. Stahl, Isolation of an autotrophic ammonia-oxidizing marine archaeon. *Nature* **437**, 543–546 (2005).
54. J. J. Middelburg, Chemoautotrophy in the ocean. *Geophys. Res. Lett.* **38**, L24604 (2011).
55. B. Bayer, R. L. Hansman, M. J. Bittner, B. E. Noriega-Ortega, J. Niggemann, T. Dittmar, G. Herndl, Ammonia-oxidizing archaea release a suite of organic compounds potentially fueling prokaryotic heterotrophy in the ocean. *Environ. Microbiol.* **21**, 4062–4075 (2019).
56. F. O. Aylward, A. E. Santoro, Heterotrophic thaumarchaea with small genomes are widespread in the dark ocean. *mSystems* **5**, e00415–e00420 (2020).
57. J. P. Bowman, The family *colwelliaceae*, in *The Prokaryotes: Gammaproteobacteria*, E. Rosenberg, E. F. DeLong, S. Lory, E. Stackenbrandt, F. Thompson, Eds. (Springer, 2014), pp. 179–195.
58. S. Freitas, S. Hatosy, J. A. Fuhrman, S. M. Huse, D. B. M. Welch, M. L. Sogin, A. C. Martiny, Global distribution and diversity of marine *Verrucomicrobia*. *ISME J.* **6**, 1499–1505 (2012).
59. M. Sebastián, J. C. Auguet, C. X. Restrepo-Ortiz, M. M. Sala, C. Marrasé, J. M. Gasol, Deep ocean prokaryotic communities are remarkably malleable when facing long-term starvation. *Environ. Microbiol.* **20**, 713–723 (2018).
60. G. J. Herndl, T. Reinthaler, Microbial control of the dark end of the biological pump. *Nat. Geosci.* **6**, 718–724 (2013).
61. N. Fierer, D. Nemergut, R. Knight, J. M. Craine, Changes through time: Integrating microorganisms into the study of succession. *Res. Microbiol.* **161**, 635–642 (2010).
62. S. Venkatachalam, I. J. Ansorge, A. Mendes, L. I. Melato, G. F. Matcher, R. A. Dorrington, A pivotal role for ocean eddies in the distribution of microbial communities across the Antarctic Circumpolar Current. *PLOS ONE* **12**, e0183400 (2017).
63. E. K. Wear, C. A. Carlson, M. J. Church, Bacterioplankton metabolism of phytoplankton lysates across a cyclone-anticyclone eddy dipole impacts the cycling of semi-labile organic matter in the photic zone. *Limnol. Oceanogr.* **65**, 1608–1622 (2020).
64. D. S. Grundle, C. R. Löscher, G. Krahmann, M. A. Altabet, H. W. Bange, J. Karstensen, A. Körtzinger, B. Fiedler, Low oxygen eddies in the eastern tropical North Atlantic: Implications for N_2O cycling. *Sci. Rep.* **7**, 1–10 (2017).
65. P. W. Boyd, H. Claustre, M. Levy, D. A. Siegel, T. Weber, Multi-faceted particle pumps drive carbon sequestration in the ocean. *Nature* **568**, 327–335 (2019).
66. F. Hammes, M. Vital, T. Egli, Critical evaluation of the volumetric "bottle effect" on microbial batch growth. *Appl. Environ. Microbiol.* **76**, 1278–1281 (2010).
67. D. A. Hutchins, K. W. Bruland, Iron-limited diatom growth and Si:N uptake ratios in a coastal upwelling regime. *Nature* **393**, 561–564 (1998).
68. M. K. Wolf, R. C. Hamme, D. Gilbert, I. Yashayaev, V. Thierry, Oxygen saturation surrounding deep water formation events in the labrador sea from Argo-O_2 data. *Glob. Biogeochem. Cycle* **32**, 635–653 (2018).
69. R. Cai, W. Zhou, C. He, K. Tang, W. Guo, Q. Shi, M. Gonsior, N. Jiao, Microbial processing of sediment-derived dissolved organic matter: Implications for its subsequent biogeochemical cycling in overlying seawater. *J. Geophys. Res. Biogeo.* **124**, 3479–3490 (2019).
70. K. Lalonde, P. Middlestead, Y. Gélinas, Automation of $^{13}C/^{12}C$ ratio measurement for freshwater and seawater DOC using high temperature combustion. *Limnol. Oceanogr. Methods* **12**, 816–829 (2014).
71. D. A. Hansell, Dissolved organic carbon reference material program. *Eos Trans. Am. Geophys. Union* **86**, 318–318 (2005).
72. T. Dittmar, B. Koch, N. Hertkorn, G. Kattner, A simple and efficient method for the solid-phase extraction of dissolved organic matter (SPE-DOM) from seawater. *Limnol. Oceanogr. Methods* **6**, 230–235 (2008).
73. A. M. Kellerman, F. Guillemette, D. C. Podgorski, G. R. Aiken, K. D. Butler, R. G. M. Spencer, Unifying concepts linking dissolved organic matter composition to persistence in aquatic ecosystems. *Environ. Sci. Technol.* **52**, 2538–2548 (2018).
74. Y. E. Corilo, EnviroOrg. Tallahassee, FL: Florida State University (2015).
75. B. P. Koch, T. Dittmar, From mass to structure: An aromaticity index for high-resolution mass data of natural organic matter. *Rapid Commun. Mass Spectrom.* **20**, 926–932 (2006).
76. J. A. O'Donnell, G. R. Aiken, K. D. Butler, F. Guillemette, D. C. Podgorski, R. G. M. Spencer, DOM composition and transformation in boreal forest soils: The effects of temperature and organic-horizon decomposition state. *J. Geophys. Res. Biogeo.* **121**, 2727–2744 (2016).
77. T. Šantl-Temkiv, K. Finster, T. Dittmar, B. M. Hansen, R. Thyrhaug, N. W. Nielsen, U. G. Karlson, Hailstones: A window into the microbial and chemical inventory of a storm cloud. *PLOS ONE* **8**, e53550 (2013).
78. D. E. LaRowe, P. Van Cappellen, Degradation of natural organic matter: A thermodynamic analysis. *Geochim. Cosmochim. Acta* **75**, 2030–2042 (2011).
79. J. A. Hawkes, J. D'Andrilli, J. N. Agar, M. P. Barrow, S. M. Berg, N. Catalán, H. Chen, R. K. Chu, R. B. Cole, T. Dittmar, R. Gavard, G. Gleixner, P. G. Hatcher, C. He, N. J. Hess, R. H. S. Hutchins, A. Ijaz, H. E. Jones, W. Kew, M. Khaksari, D. C. Palacio Lozano, J. Lv, L. R. Mazzoleni, B. E. Noriega-Ortega, H. Osterholz, N. Radoman, C. K. Remucal, N. D. Schmitt, S. K. Schum, Q. Shi, C. Simon, G. Singer, R. L. Sleighter, A. Stubbins, M. J. Thomas, N. Tolic, S. Zhang, P. Zito, D. C. Podgorski, An international laboratory comparison of dissolved organic matter composition by high resolution mass spectrometry: Are we getting the same answer? *Limnol. Oceanogr. Methods* **18**, 235–258 (2020).
80. R. LaBrie, J. F. Lapierre, R. Maranger, Contrasting patterns of labile and semilabile dissolved organic carbon from continental waters to the open ocean. *J. Geophys. Res. Biogeosci.* **125**, e2019JG005300 (2020).
81. R. LaBrie, N. Fortin St-Gelais, S. Bélanger. paRafac_correction: A R Package to corrects EEMs and derive CDOM and FDOM indices (v1.0.3). (Zenodo, 2017); https://doi.org/10.5281/zenodo.832320.
82. T. Ohno, Fluorescence inner-filtering correction for determining the humification index of dissolved organic matter. *Environ. Sci. Technol.* **36**, 742–746 (2002).
83. K. R. Murphy, C. A. Stedmon, D. Graeber, R. Bro, Fluorescence spectroscopy and multi-way techniques. PARAFAC. *Anal. Methods* **5**, 6557–6566 (2013).
84. A. M. Comeau, G. M. Douglas, M. G. I. Langille, Microbiome helper: A custom and streamlined workflow for microbiome research. *MSystems* **2**, e00127-16 (2017).
85. A. M. Comeau, W. K. W. Li, J.-É. Tremblay, E. C. Carmack, C. Lovejoy, Arctic ocean microbial community structure before and after the 2007 record sea ice minimum. *PLOS ONE* **6**, e27492 (2011).
86. B. J. Callahan, P. J. McMurdie, M. J. Rosen, A. W. Han, A. J. A. Johnson, S. P. Holmes, DADA2: High-resolution sample inference from Illumina amplicon data. *Nat. Methods* **13**, 581 (2016).
87. D. C. Smith, F. Azam, A simple, economical method for measuring bacterial protein synthesis rates in seawater using 3H-leucine. *Marine Microb. Food Webs* **6**, 107–114 (1992).
88. M. Simon, F. Azam, Protein content and protein synthesis rates of planktonic marine bacteria. *Mar. Ecol. Prog. Ser.* **51**, 201–213 (1989).
89. C. Belzile, S. Brugel, C. Nozais, Y. Gratton, S. Demers, Variations of the abundance and nucleic acid content of heterotrophic bacteria in Beaufort Shelf waters during winter and spring. *J. Mar. Syst.* **74**, 946–956 (2008).
90. J. Oksanen, F. G. Blanchet, R. Kindt, P. Legendre, R. B. O'hara, G. L. Simpson, P. Solymos, M. H. H. Stevens, H. Wagner, Vegan: Community ecology package. R package version 1.17-4 (2010); http://CRAN.R-project.org/package=vegan.
91. R Core Team (Vienna, Austria: R Foundation for Statistical Computing, 2017); www.R-project.org/.
92. S. Groeskamp, J. H. LaCasce, T. J. McDougall, M. Rogé, Full-depth global estimates of ocean mesoscale eddy mixing from observations and theory. *Geophys. Res. Lett.* **47**, e2020GL089425 (2020).

Acknowledgments: We thank the crew members of the CCGS Hudson, N. Rene (Brooklyn College-CUNY) for technical help, and M. Botrel and J. F. Lapierre (UdeM) for constructive comments at different stages of the project. **Funding:** This work was largely supported by a NSERC- Climate Change and Atmospheric Research (CCAR) to the Ventilation, Interactions and Transports Across the Labrador Sea (VITALS) program and NSERC Discovery to R.M. and an UdeM and FRQNT student scholarship to R.L. Collection and analysis of oceanographic observations in the Labrador Sea were done in support of the Deep-Ocean Observation and Research Synthesis (DOORS) initiated and led by I.Y. A portion of this work was performed at the National High Magnetic Field Laboratory ICR User Facility, which is supported by the National Science Foundation Division of Chemistry through DMR-1157490 and DMR-1644779 and the State of Florida. **Author contributions:** R.L. did the field and laboratory work and data analysis, wrote the first draft, edited the manuscript, and contributed study design. B.P. contributed laboratory work, data analysis, and manuscript editing. N.F.S.-G. contributed data analysis and manuscript editing. I.Y. contributed field work, data analysis, and manuscript editing. J.C., Y.G., and L.T. contributed data and edited the manuscript. R.G.M.S. contributed data and manuscript editing. F.G. and D.C.P. contributed laboratory work and manuscript editing. R.M. designed the study, contributed data analysis, and cowrote and edited the manuscript. **Competing interests:** The authors declare that they have no competing interests. **Data and materials availability:** All data and scripts are available at www.github.com/LaboMaranger/MCP and at https://doi.org/10.5281/zenodo.6578278. All data needed to evaluate the conclusions in the paper are present in the paper and/or the Supplementary Materials.

Submitted 27 October 2021
Accepted 24 May 2022
Published 8 July 2022
10.1126/sciadv.abn0035

ScienceAdvances

Deep ocean microbial communities produce more stable dissolved organic matter through the succession of rare prokaryotes

Richard LaBrieBérangère PéquinNicolas Fortin St-GelaisIgor YashayaevJennifer CherrierYves GélinasFrançois GuillemetteDavid C. PodgorskiRobert G. M. SpencerLuc TremblayRoxane Maranger

Sci. Adv., 8 (27), eabn0035. • DOI: 10.1126/sciadv.abn0035

Science Advances (ISSN) is published by the American Association for the Advancement of Science. 1200 New York Avenue NW, Washington, DC 20005. The title *Science Advances* is a registered trademark of AAAS.